Communications

Fast Frequency-Sweep Analysis of RF Coils for MRI

Dan Jiao and Jian-Ming Jin*

***Abstract*—A fast frequency-sweep technique is developed for the analysis of radio-frequency coils for magnetic resonance imaging. This technique applies the method of asymptotic waveform evaluation to the moment method solution of the integral equation for the original physical problem. Numerical examples show that the proposed technique can speed up the analysis by more than an order of magnitude.**

***Index Terms*—Asymptotic waveform evaluation (AWE), magnetic resonance imaging (MRI), method of moments (MoM), radio-frequency (RF) coils.**

I. Introduction

The radio-frequency (RF) coil is an important device in a magnetic resonance imaging (MRI) system. The primary method used for its analysis and design is based on the equivalent lumped-circuit model [1]–[5]. In this method, whose details are described in a recent book [6], the conductors used to construct an RF coil are modeled as inductors and the RF coil is then modeled as an LC network. The Kirchhoff voltage and current laws are then employed to establish a set of linear equations, whose solution gives the resonant frequencies and the current distributions in the coil. The method is simple and also effective for RF coils operating at a low frequency. However, by modeling a conductor as an inductor, one neglects the current variation in the conductor and also the radiation loss of the conductor. This introduces a significant error in the analysis of RF coils operating at higher frequencies. As a result, the equivalent lumped-circuit method becomes inaccurate and often predicts the current distribution that disagrees with measured data.

A more accurate analysis of RF coils is to employ the method of moments (MoM) [7], which is based on the exact solution of Maxwell's equations. This analysis is valid at both low and high frequencies and it is also applicable to complex RF coils having structures such as RF shields and end-caps. Recently, the MoM has been used for the analysis and design of RF coils for MRI [8]–[11]. With the MoM, the analysis is performed at a specified frequency. Since RF coils are highly resonant devices, the analysis must be repeated at many frequencies with a very small frequency increment in order to obtain the frequency response of an RF coil. This results in an excessively long computing time, especially when many designs have to be evaluated.

In this paper, we describe a fast frequency-sweep technique to alleviate this problem. This technique applies the method of asymptotic waveform evaluation (AWE) [12], [13] to the MoM solution of the integral equation for the RF coil analysis. Numerical examples show that the proposed technique can speed up the analysis by more than an order of magnitude.

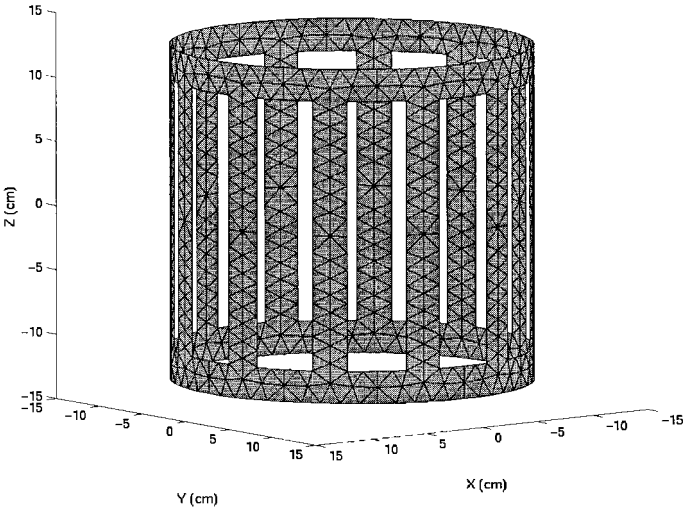

Fig. 1. Subdivision of a birdcage RF coil into small triangular elements (Capacitors are not shown).

II. Formulation

Consider an RF coil made of conducting strips[1] and lumped capacitors and possibly enclosed in an RF shield. A voltage source applied to the coil will induce an electric current in the coil and the shield. The electric field intensity produced by this current can be expressed as

$$\boldsymbol{E}(\boldsymbol{r}) = -jk\eta \int\int_S \overline{\boldsymbol{G}}(\boldsymbol{r}, \boldsymbol{r}') \cdot \boldsymbol{J}(\boldsymbol{r}')\, d\boldsymbol{r}' \tag{1}$$

where k is the free-space wavenumber, η is the free-space wave impedance, S denotes the conducting surface of the coil and the shield, $\boldsymbol{J}$ denotes the unknown surface current density on S, and $\overline{\boldsymbol{G}}(\boldsymbol{r}, \boldsymbol{r}')$ is the well-known free-space dyadic Green's function given by

$$\overline{\boldsymbol{G}}(\boldsymbol{r}, \boldsymbol{r}') = \left(\overline{\boldsymbol{I}} + \frac{\nabla\nabla}{k^2}\right) g(\boldsymbol{r}, \boldsymbol{r}'), \qquad g(\boldsymbol{r}, \boldsymbol{r}') = \frac{e^{-jk|\boldsymbol{r}-\boldsymbol{r}'|}}{4\pi|\boldsymbol{r}-\boldsymbol{r}'|}$$

with $\overline{\boldsymbol{I}}$ being the unit dyad.

To determine the unknown surface current density $\boldsymbol{J}$, we first subdivide the conducting surface S into small triangular elements. One example of such a subdivision is shown in Fig. 1. The surface current density can then be expanded using the Rao–Wilton–Glisson

Manuscript received April 30, 1999; revised June 23, 1999. This work was supported by the National Science Foundation (NSF) under Grant ECE 94-57735. *Asterisk indicates corresponding author*

D. Jiao is with the Center for Computational Electromagnetics, Department of Electrical and Computer Engineering, University of Illinois at Urbana-Champaign, Urbana, IL 61801-2991 USA.

*J. M. Jin is with the Center for Computational Electromagnetics, Department of Electrical and Computer Engineering, University of Illinois at Urbana-Champaign, 1406 West Green Street, Urbana, IL 61801-2991 USA (e-mail: j-jin1@uiuc.edu)

Publisher Item Identifier S 0018-9294(99)07648-X.

[1]The moment method analysis of RF coils made of circular conducting wires is described in detail in a recent book [6]. A narrow strip of width w is equivalent to a circular wire with a radius given by $a = 0.223\ w$. This equivalence is derived by equating the self-impedance of a strip segment to that of a wire segment of the same length. Hence, a moment method solution based on strips can be applied to RF coils made of wires, and *vice versa*.

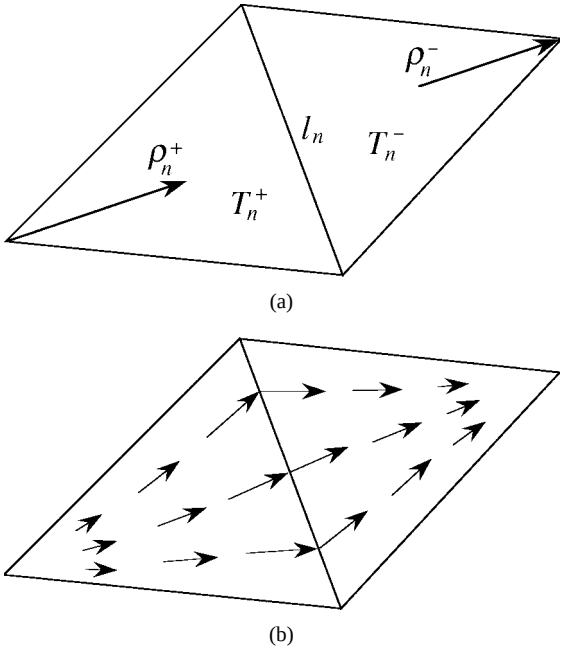

Fig. 2. (a) Illustration of two joint triangular elements. (b) Vector plot of the RWG function $\boldsymbol{f}_n$.

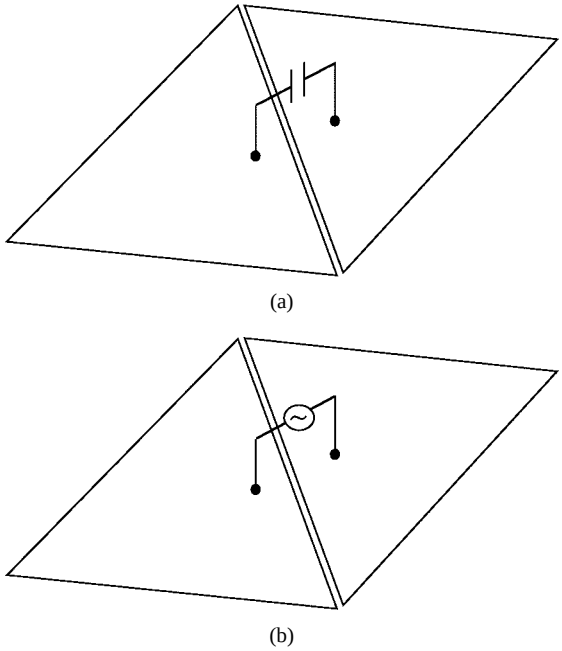

Fig. 3. (a) A capacitor applied at T_m. (b) A voltage source applied at T_m.

(RWG) basis function $\boldsymbol{f}_n(\boldsymbol{r})$ [14]

$$\boldsymbol{J}(\boldsymbol{r}) = \sum_{n=1}^{N} I_n \boldsymbol{f}_n(\boldsymbol{r}) \tag{2}$$

where N is the number of unknowns, which is the number of edges shared by two triangular elements, and I_n denotes the unknown expansion coefficient. The RWG basis function $\boldsymbol{f}_n(\boldsymbol{r})$, also known as the triangular roof-top function, is defined over two triangular elements joined at a common edge ℓ_n

$$\boldsymbol{f}_n(\boldsymbol{r}) = \begin{cases} \dfrac{\ell_n}{2A_n^+}\boldsymbol{\rho}_n^+, & \boldsymbol{r} \text{ in } T_n^+ \\ \dfrac{\ell_n}{2A_n^-}\boldsymbol{\rho}_n^-, & \boldsymbol{r} \text{ in } T_n^- \\ 0, & \text{otherwise} \end{cases} \tag{3}$$

where $T_n^{\pm}$ denote the two triangles associated with the nth edge, $A_n^{\pm}$ are the areas of triangles $T_n^{\pm}$, ℓ_n is the length of the nth edge, and $\boldsymbol{\rho}_n^{\pm}$ are the vectors defined in Fig. 2(a). The vector plot of $\boldsymbol{f}_n(\boldsymbol{r})$ is illustrated in Fig. 2(b). The most important feature of this basis function is that its normal component to edge ℓ_n is a constant (normalized to one) whereas the normal components to other edges are zero. This feature guarantees the continuity of current flow over all edges and makes I_n the current density passing through edge ℓ_n. Triangular elements are chosen here because of their excellent modeling capability of arbitrary geometries, which is not shared by rectangular elements.

Applying Galerkin's method to (1) results in a matrix equation

$$Z(k)I(k) = V(k) \tag{4}$$

in which the impedance matrix Z and vector V have the elements given by

$$Z_{mn}(k) = jk\eta \iint_{T_m}\iint_{T_n} \left[\boldsymbol{f}_m(\boldsymbol{r})\cdot\boldsymbol{f}_n(\boldsymbol{r}') - \frac{1}{k^2}\nabla \cdot \boldsymbol{f}_m(\boldsymbol{r})\nabla\cdot\boldsymbol{f}_n(\boldsymbol{r}')\right] g(\boldsymbol{r},\boldsymbol{r}')\,d\boldsymbol{r}'\,d\boldsymbol{r} \tag{5}$$

$$V_m(k) = -\iint_{T_m} \boldsymbol{E}(\boldsymbol{r})\cdot\boldsymbol{f}_m(\boldsymbol{r})\,d\boldsymbol{r} \tag{6}$$

where T_m and T_n denote the support of $\boldsymbol{f}_m$ and $\boldsymbol{f}_n$, respectively.

If there is neither a capacitor nor a voltage source applied at T_m, then $V_m(k) = 0$ because the boundary condition requires that the tangential electric field must vanish on a perfectly conducting surface (see Appendix for a more general case). If a capacitor C_m is applied at T_m, as illustrated in Fig. 3(a), it is easy to find that

$$V_m(k) = -\frac{(\ell_m)^2}{j\omega C_m} I_m(k) \tag{7}$$

where ω denotes the angular frequency. Clearly, this can be moved to the left-hand side of (4), which is equivalent to adding $(\ell_m)^2/j\omega C_m$ to Z_{mm}. If a voltage source V_m^{ex} is applied at T_m, as illustrated in Fig. 3(b), then

$$V_m(k) = \ell_m V_m^{ex} \tag{8}$$

which provides the right-hand side of (4) for a solution of $I(k)$.

To obtain the solution of (4) over a wide frequency band, we expand $I(k)$ into a Taylor series

$$I(k) = \sum_{n=0}^{Q} m_n (k-k_0)^n \tag{9}$$

where k_0 is the expansion point. Substituting this into (4), expanding the impedance matrix $Z(k)$ and the excitation vector $V(k)$ into a Taylor series, and finally matching the coefficients of the equal powers of $k-k_0$ on both sides yield the recursive relation for the moment vectors

$$m_0 = Z^{-1}(k_0)V(k_0) \tag{10}$$

$$m_n = Z^{-1}(k_0)\left[\frac{V^{(n)}(k_0)}{n!} - \sum_{i=1}^{n}\frac{Z^{(i)}(k_0)m_{n-i}}{i!}\right] \quad n \geq 1 \tag{11}$$

where $Z^{(i)}$ denotes the ith derivative of $Z(k)$ and likewise $V^{(n)}$ denotes the nth derivative of $V(k)$. These derivatives are found

TABLE I
CPU TIMINGS FOR CALCULATIONS ON DIGITAL PERSONAL WORKSTATION

Problem	Number of elements	Number of unknowns	AWE method		Direct method		Speed-up
			Freq. pts.	CPU time	Freq. pts.	CPU time	
Fig. 4	336	348	25 000	35.6 s	250	1352 s	38.0
Fig. 5	818	1043	20 000	719.5 s	400	36 192 s	50.3

analytically in this work using the following derivative formula. Given a function

$$f(k) = (1 - ck^2)\frac{e^{-jkr}}{r}$$

where c is a constant, its nth derivative is given by

$$f^{(n)}(k) = [jn(n-1) + 2nkr]ce^{-jkr}(-jr)^{n-3} - \left(1 - ck^2\right)re^{-jkr}(-jr)^{n-2}.$$

The Taylor expansion has a limited bandwidth. To obtain a wider bandwidth, we represent $I(k)$ with a better behaved rational Padé function

$$I(k) = \frac{\sum_{i=0}^{L} a_i(k-k_0)^i}{1 + \sum_{j=1}^{M} b_j(k-k_0)^j} \tag{12}$$

where $L + M = Q$. The unknown coefficients a_i and b_j can be calculated by substituting (9) into (12), multiplying (12) with the denominator of the Padé expansion, and matching the coefficients of the equal powers of $k - k_0$. This leads to the matrix equation

$$\begin{bmatrix} m_L & m_{L-1} & m_{L-2} & \cdots & m_{L-M+1} \\ m_{L+1} & m_L & m_{L-1} & \cdots & m_{L-M+2} \\ m_{L+2} & m_{L+1} & m_L & \cdots & m_{L-M+3} \\ \vdots & \vdots & \vdots & \ddots & \vdots \\ m_{L+M-1} & m_{L+M-2} & m_{L+M-3} & \cdots & m_L \end{bmatrix} \begin{bmatrix} b_1 \\ b_2 \\ b_3 \\ \vdots \\ b_M \end{bmatrix} = - \begin{bmatrix} m_{L+1} \\ m_{L+2} \\ m_{L+3} \\ \vdots \\ m_{L+M} \end{bmatrix} \tag{13}$$

which can be solved for b_j. Once b_j are obtained, the unknown coefficients a_i can then be calculated as

$$a_i = \sum_{j=0}^{i} b_j m_{i-j} \qquad 0 \le i \le L. \tag{14}$$

Clearly, in the procedure described above the impedance matrix $Z(k)$ is inverted only once, which is the main reason for the efficiency of the AWE method. In the case that one expansion point is not sufficient to cover the desired frequency band, one can use multipole expansion points, which can be selected automatically using a simple binary search algorithm [15].

III. NUMERICAL EXAMPLES

To demonstrate the efficiency and accuracy of the proposed method, a number of numerical examples are considered. We first applied the method to a 2.25 cm × 2.25 cm square loop made of a 0.143-cm-wide strip and connected to a capacitor of 90 pF [6, p. 145]. The calculated resonant frequency agrees very well with the measured value with a relative error less than 2.3%. We then applied the method to a dipole antenna made of a conducting strip, the calculated input impedance as a function of frequency agrees very well with other solutions [7, p. 72] with the largest relative error less than 5%.

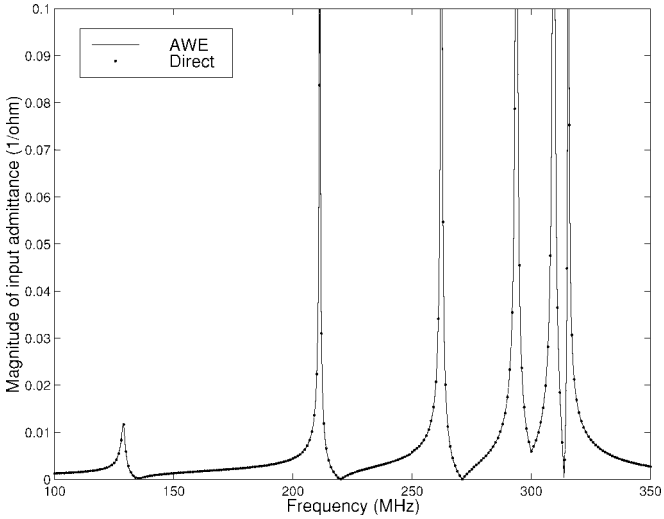

Fig. 4. Magnitude of the input admittance of a nonshielded low-pass birdcage coil as a function of frequency.

Having verified the method, we applied it to a low-pass birdcage coil whose diameter and length are 26 cm. The coil is made of 2.54-cm-wide conducting strips and the number of rungs is 12. The capacitors have a value of 1.7 pF to place the dominant mode at 128 MHz and the voltage is applied across one of the capacitors. Fig. 4 shows the magnitude of the input admittance as a function of frequency. The number of triangular elements used to model the coil is 336 and the number of unknowns is 348. With a frequency increment of 1 MHz, it takes the direct method, which solves (4) repeatedly for each frequency, 1352 s to obtain the solution on a digital personal workstation (500-MHz Alpha 21164 processor). With a sixth-order Taylor expansion ($Q = 6$, $L = 3$, $M = 3$), the AWE method produces an accurate solution with 0.01-MHz increments over the entire band in 35.6 s, which is a speed-up of 38. A higher-order Taylor expansion would result in an even larger speed-up at the expense of an increased computer memory requirement.

The above calculations are repeated for the birdcage coil placed in an RF shield having a diameter of 32 cm and a length of 30 cm. The capacitors have a value of 2.95 pF to place the dominant mode at 128 MHz. Fig. 5 gives the magnitude of the input admittance as a function of frequency. The discretization and CPU time information is summarized in Table I, which shows a similar speed-up.

IV. CONCLUSION

In this paper, we described a fast frequency-sweep technique for the analysis of RF coils for MRI. This technique applies the AWE

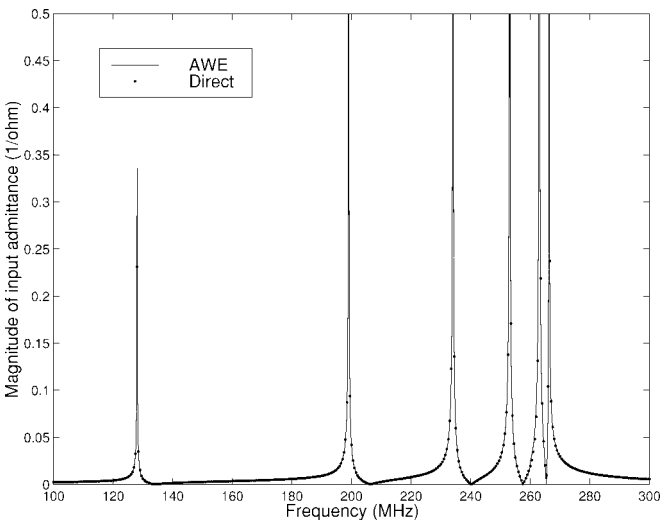

Fig. 5. Magnitude of the input admittance of a shielded low-pass birdcage coil as a function of frequency.

method to the MoM solution of the integral equation for the RF coil. Numerical examples showed that the proposed technique can speed up the analysis by more than an order of magnitude, making it a very useful tool for the design of RF coils.

APPENDIX

If the conduction loss of a coil has to be evaluated, the coil must be considered as a nonperfect conductor. In this case, even if there is neither a capacitor nor a voltage source applied at T_m, $V_m(k) \neq 0$. Instead, since $\boldsymbol{E} = \rho \boldsymbol{J}$ with ρ being the surface resistivity, (6) becomes

$$V_m(k) = -\rho \sum_{n=1}^{N} I_n(k) \int\int_{T_m} \boldsymbol{f}_m(\boldsymbol{r}) \cdot \boldsymbol{f}_n(\boldsymbol{r})\, d\boldsymbol{r}. \tag{15}$$

Clearly, this can be moved to the left-hand side of (4), which is equivalent to adding $\rho \int\int_{T_m} \boldsymbol{f}_m(\boldsymbol{r}) \cdot \boldsymbol{f}_n(\boldsymbol{r})\, d\boldsymbol{r}$ into Z_{mn}. Note that this integral vanishes when T_m and T_n do not overlap each other.

REFERENCES

[1] C. E. Hayes, W. A. Edelstein, J. F. Schenck, O. M. Mueller, and M. Eash, "An efficient, highly homogeneous radiofrequency coil for whole-body NMR imaging at 1.5 T," *J. Magn. Reson.*, vol. 63, pp. 622–628, 1985.

[2] J. Tropp, "The theory of the bird-cage resonator," *J. Magn. Reson.*, vol. 82, pp. 51–62, 1989.

[3] P. M. Joseph and D. Lu, "A technique for double resonant operation of birdcage imaging coils," *IEEE Trans. Med. Imag.*, vol. 8, pp. 286–294, Sept. 1989.

[4] J. M. Jin, G. Shen, and T. Perkins, "On the field inhomogeneity of birdcage coils," *Magn. Reson. Med.*, vol. 32, pp. 418–422, 1994.

[5] J. M. Jin, R. L. Magin, G. Shen, and T. Perkins, "A simple method to incorporate the effects of an RF shield into RF resonator analysis for MRI applications," *IEEE Trans. Biomed. Eng.*, vol. 42, pp. 840–843, Aug. 1995.

[6] J. M. Jin, *Electromagnetic Analysis and Design in Magnetic Resonance Imaging.* Boca Raton, FL: CRC, 1998.

[7] R. F. Harrington, *Field Computation by Moment Methods.* New York: IEEE Press, 1993.

[8] S. M. Wright, "Moment method analysis of coupled RF coils," in *Works in Progress, 11th Annu. Sci. Mtg. Soc. Magn. Reson. Med.*, p. 4015, 1992.

[9] H. Ochi, E. Yamamoto, K. Sawaya, and S. Adachi, "Analysis of magnetic resonance imaging antenna inside an RF shield," *Electron. Commun. Japan*, Part 1, vol. 77, pp. 37–44, 1994.

[10] J. Chen, Z. Feng, and J. M. Jin, "Numerical simulation of SAR and B_1-field inhomogeneity of shielded RF coils loaded with the human head," *IEEE Trans. Biomed. Eng.*, vol. 45, pp. 650–659, May 1998.

[11] H. Fujita, "RF coil optimization using the method of moments," in *Proc. Workshop Computational Electromagnetics in Magnetic Resonance*, College Station, TX, May 30–June 1, 1998.

[12] L. T. Pillage and R. A. Rohrer, "Asymptotic waveform evaluation for timing analysis," *IEEE Trans. Computer-Aided Design*, vol. 9, pp. 352–366, Apr. 1990.

[13] E. Chiprout and M. Nakhla, *Asymptotic Waveform Evaluation and Moment Matching for Interconnect Analysis.* Boston, MA: Kluwer Academic, 1994.

[14] S. M. Rao, D. R. Wilton, and A. W. Glisson, "Electromagnetic scattering by surface of arbitrary shape," *IEEE Trans. Antennas Propagat.*, vol. AP-30, pp. 409–418, 1982.

[15] J. Zhang and J. M. Jin, "Preliminary study of AWE for FEM analysis of scattering problems," *Microwave Opt. Tech. Lett.*, vol. 17, pp. 7–12, 1998.